

Osteopontin Upregulates Col IV Expression by Repressing miR-29a in Human Retinal Capillary Endothelial Cells

Ping Duan,^{1,2,3} Siyu Chen,^{1,2,3} Yuxiao Zeng,^{1,2} Haiwei Xu,^{1,2} and Yong Liu^{1,2}

¹Southwest Hospital, Southwest Eye Hospital, Third Military Medical University (Amy Medical University), Chongqing 400038, China; ²Key Lab of Visual Damage and Regeneration and Restoration of Chongqing, Chongqing 400038, China

Abnormal synthesis of extracellular matrix (ECM), especially collagen type IV (Col IV), in human retinal capillary endothelial cells (HRCECs) and resultant basement membrane (BM) thickening is the most prominent and characteristic feature of early diabetic retinopathy (DR). Osteopontin (OPN) has been shown to play an important role in the pathogenesis of DR and specifically, found to be critically involved in diabetic nephropathy, as it can upregulate many factors, like collagen IV. However, the precise role of OPN in the pathogenesis of DR and the underlying mechanisms remain unclear. In this study, 51 differentially expressed microRNAs (miRNAs; 42 miRNAs upregulated and 9 miRNAs downregulated) were first identified in retina of streptozotocin (STZ)-induced diabetic mice with DR. Among these miRNAs, we identified miRNA (miR)-29a as a prominent miRNA that targeted and directly downregulated Col IV expression through database prediction and dual-luciferase reporter assay, which was further confirmed in HRCECs using miR-29a mimic, miR-29a inhibitor, and pre-miR-29a transfection. Furthermore, OPN upregulated Col IV expression via a miR-29a-repressed pathway in HRCECs. Taken together, these results provided a miR-29a-repressing mechanism through which OPN plays roles in abnormal synthesis of Col IV in HRCECs and resultant BM thickening, contributing to the pathogenesis of DR.

INTRODUCTION

Diabetic retinopathy (DR) is one of the most common microcapillary complications of diabetes and the main cause of visual disability and blindness among adults of working age (20–65 years old).¹ In the early stage of DR, human retinal capillary endothelial cells (HRCECs) and retinal pigment epithelial (RPE) cells are impaired by adverse effects of high glucose (HG). Another important histological hallmark of DR is the thickening of retinal capillary basement membranes (BMs).^{2,3} BMs are present at the surface of HRCECs and are comprised of approximately 30 high-molecular glycoproteins that either polymerize or bind to other BM proteins to form thin extracellular matrix (ECM) sheets.^{4,5} Collagen IV (Col IV) is the main component of the retinal capillary BMs, and elevated levels of Col IV in serum and urine have been associated with diabetic microangiopathic complications, especially in diabetic nephropathy (DN).^{6–8} In-

hibition of collagen metabolism, especially for collagen IV synthesis, has demonstrated antiangiogenic features for potential application in many diseases, including DN.⁹ Nevertheless, the important factors that stimulate collagen IV expression in the retinal capillary BMs remain largely unknown.

Osteopontin (OPN), also known as secreted phospho-protein 1 (SPP1), is a multifunctional extracellular matrix glycoprotein and exhibits diverse functions involved in capillary complication of diabetes, such as angiogenesis, inflammation, and fibrosis.^{10,11} The relationship between plasma OPN levels and DR has been explored. Whereas one study found a positive but nonstatistically significant relationship,¹² another study found a positive and statistically significant relationship.¹³ Additionally, several studies measured OPN levels in the vitreous fluid and consistently demonstrated higher levels of OPN in patients with DR when compared to diabetic patients without DR.¹⁴ These studies suggest that OPN may play an important role in the pathogenesis of DR and represent an organ-specific biomarker. Interestingly, OPN appears to play an important role in mediating collagen IV synthesis found in a hyperglycemic environment,¹⁵ and especially, OPN has been found to be critically involved in diabetic nephropathy, as it can upregulate many factors, like collagen IV.¹⁶ However, the precise role of OPN in the pathogenesis of DR and the underlying mechanisms remain unclear.

The pathogenesis of DR is extremely complicated, and numerous hyperglycemia-linked pathways have been investigated. Recently, enormous numbers of noncoding RNAs (ncRNAs), especially microRNAs (miRNAs), were found to express and play critical roles in the progression of DR.^{17,18} miRNAs are a group of short (21–23 nucleotides), highly conserved endogenous RNAs that do not encode proteins but

Received 19 October 2019; accepted 5 February 2020;
<https://doi.org/10.1016/j.omtn.2020.02.001>.

³These authors contributed equally to this work.

Correspondence: Haiwei Xu, Southwest Hospital, Southwest Eye Hospital, Third Military Medical University (Amy Medical University), Chongqing 40038, China. E-mail: haiweixu2001@163.com

Correspondence: Yong Liu, Southwest Hospital, Southwest Eye Hospital, Third Military Medical University (Amy Medical University), Chongqing 40038, China. E-mail: liuyy99@163.com



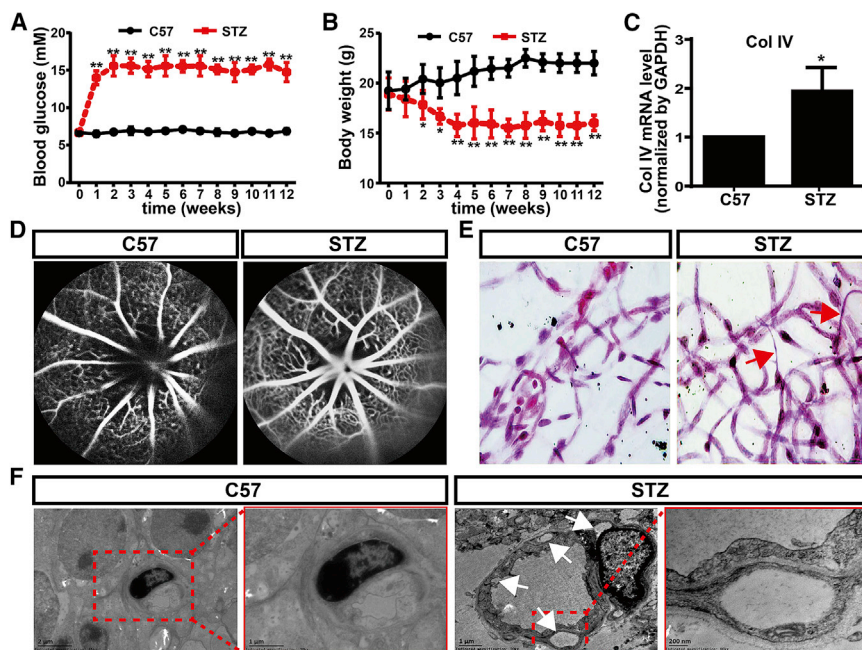


Figure 1. STZ-Induced Diabetic Model with DR

(A and B) Effects of streptozotocin (STZ) on blood glucose (A) and body weight (B) levels of C57BL/6 mice. (C) The expressions of Col IV in retinas of C57 and STZ-induced diabetic mice were examined by quantitative real-time PCR. N = 4 per group; * $p < 0.05$, STZ group versus C57 group. (D) Fluorescein fundus angiography (FFA) of C57 and STZ-induced diabetic mice. (E) Retinal capillaries of C57 and STZ-induced diabetic mice were shown by hematoxylin and PAS staining. Arrows point to acellular capillaries. (F) TEM of retinal capillaries of C57 and STZ-induced diabetic mice. Arrows point to cavity-like structures.

abnormal compared with those in control C57 mice. Normally, there was no acellular capillary in retina of control C57 mice; however, abundant acellular vessels were observed in retina of STZ-induced diabetic mice (Figure 1E). Furthermore, transmission electron microscope (TEM) analysis showed abnormal retinal capillary with abundant cavity-like structures in retina of STZ-induced diabetic mice (Figure 1F).

Taken together, these results indicate a successful STZ-induced diabetic model with DR.

modulate gene expression via inducing mRNA degradation or inhibiting protein translation by binding through partial sequence homology to the sites in the 3' untranslated region (3' UTR) of target mRNAs.¹⁹ Notably, miRNAs have emerged as regulators involved in critical biologic processes, such as migration, apoptosis, proliferation, and DR-related neo-capillarization.¹⁷ This study was designed to explore the role of OPN in the thickening of BMs in DR, and the results showed that OPN upregulated the expression of ECM protein Col IV by inhibiting miR-29a in HRCECs.

RESULTS

Generation of STZ-Induced Diabetic Mice with DR

Diabetes was induced by a consecutive intraperitoneal injection of streptozotocin (STZ; 60 mg/mL) for 5 days. At 7 days after the first injection, blood glucose level increased from 6.80 ± 0.18 mM to 14.65 ± 1.13 mM. The blood glucose level reached at 15.78 ± 1.68 mM at 14 days, and the high blood glucose level maintained for more than 12 weeks (Figure 1A). The blood glucose level of control C57BL/6 (C57) mice remained relatively constant throughout this period. Additionally, the control C57 mice maintained body weights of linear growth. In contrast, the body weights of STZ-induced diabetic mice decreased significantly compared with those of control C57 mice (Figure 1B), suggesting a successful development of the STZ-induced diabetic model. Consistent with a previous study,²⁰ the elevated mRNA level of Col IV was found in retina of STZ-induced diabetic mice (Figure 1C). Furthermore, we performed fluorescein fundus angiography (FFA) to observe retinal microcapillary permeability. Obvious leakage at optic disc was found in STZ-induced diabetic mice, whereas no leakage was detected in control C57 mice (Figure 1D). Periodic acid–Schiff (PAS) staining showed that retinal capillaries of STZ-induced diabetic mice were strikingly

Retinal Small RNA Sequencing

To explore the role of miRNAs in the pathogenesis of DR, retinal small RNAs of C57 and STZ-induced diabetic mice were sequenced, and more than 1,000 miRNAs and about 190 piwi-interacting RNAs (piRNAs) were expressed in retina (Table S1). The length of these small RNAs is between 18 nt and 30 nt, and 94.4% of these small RNAs were miRNAs. Among these miRNAs, 71.4% were mature miRNAs, and 28.6% were miRNA precursors (Figures 2A and 2B). Differentially expressed small RNAs (DES) between C57 and STZ-induced retinal samples were searched for by DEGseq and ExpDiff methods. 51 differentially expressed miRNAs were identified, in which 42 miRNAs were upregulated, and 9 miRNAs were downregulated in retina of STZ-induced diabetic mice (Figure 2C; Table S2).

Multiple software programs were used to predict candidate target genes of differentially expressed miRNAs, and more than 20,000 extract intersections of predicted targets were found (Figure 2D). The main biological functions of these predicted targets and the molecular pathways were then assessed using Kyoto Encyclopedia of Genes and Genomes (KEGG) pathway enrichment analysis and Gene Ontology (GO) enrichment analysis. The results showed that these predicted targets were enriched in several key signaling pathway-related networks and biological functions, including cyclic AMP (cAMP) signaling pathway, calcium signaling pathway, oxytocin signaling pathway, capillary smooth muscle contraction, and type II diabetes mellitus (Figure S1). Furthermore, 20 extracellular matrix transcripts of cellular component involved in basement membranes were included in these predicted targets (Figure S2).

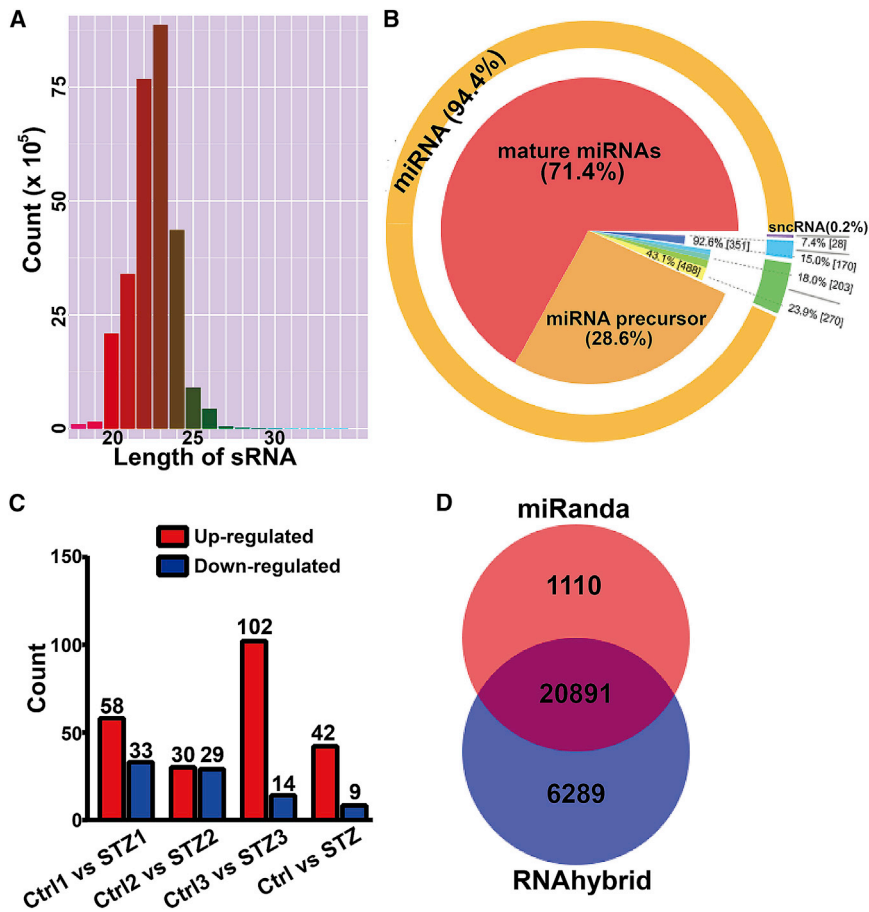


Figure 2. Small RNA Sequencing of Retinas from Control C57 and STZ-Induced Diabetic Mice

(A) Length distribution of small RNAs (sRNA). The length distribution analysis is helpful to see the compositions of the sRNA sample. (B) The proportion of different kinds of sRNA. (C) Differentially expressed miRNA. (D) Predicted targets of differentially expressed miRNA.

several species. The 3' UTR of Col4a1 mRNA contains an 8-mer (UGGUGCUA, position 30–37) and a 7-mer (GGUGCUA, position 308–314), which are complementary to the seed regions of miR-29 (Figures 3A and 3B). The two conserved binding sites were also found in other transcripts of Col I and Col IV (Figure 3C; Table S4). Furthermore, the increased expression of miR-29a in retina of STZ-induced diabetic mice was validated by quantitative real-time PCR (Figure 3D).

Col IV Is a Target of miR-29a

To provide functional validation of the targets of miR-29 for Col IV mRNAs, we performed a dual-luciferase reporter assay by inserting the 3' UTR sequence of Col IV (Col4a1) downstream of the renilla luciferase reporter in the pSI-check2 vector (Figure 4A). Compared with cotransfection of scrambled miRNA with wild-type Col4a1 3' UTR (Col IV WT), cotransfection of hsa-miR-29a with wild-type Col4a1 3'

UTR resulted in a significant repression of luciferase reporter activity in HEK293T cells (Figure 4D). To demonstrate further the specificity of miR-29a for the binding sites, we generated three mutants of Col4a1 transcript, where the 3' UTR binding sites of miR-29a TGGTGCTA were mutated into AGCTCCGA (mut1), or GGTGCTA was mutated into CGAGATC (mut2) or both (mut1 + mut2) (Figures 4B and 4C). mut1 and mut2 could slightly increase luciferase reporter activity, and both mutations (mut1 + mut2) within the binding sites of Col4a1 mRNAs significantly abrogated the effect of miR-29a (Figure 4D). Taken together, these data confirm that miR-29a directly targets and inhibits Col4a1 expression by binding the 3' UTR binding sites of Col4a1 mRNA and repressing its translation.

miR-29a Directly Regulates Col IV Expression in HRCECs

To provide further evidence that Col4a1 is a target of miR-29a in HRCECs, we transfected HRCECs with miR-29a mimic or inhibitor. With the use of quantitative real-time PCR analysis, we confirmed that the expression of miR-29a with miR-29a mimic transfection was significantly higher than that with control scrambled miRNA transfection (Figure 5A). In contrast, miR-29a inhibitor transfection decreased the expression of miR-29a (Figure 5B). Compared with the control scrambled miRNA-transfected HRCECs, an increased mRNA level of Col IV was found in the miR-29a inhibitor-transfected

Analysis of Differentially Expressed miRNAs

Next, we screened different databases to select miRNA candidates that were potentially involved in diabetes mellitus, DR, and collagen synthesis. A number of miRNAs (miR-10, miR-17, miR-34, miR-144, miR-190, miR-199, miR-200, miR-216, and miR-219),¹⁷ proved to be involved in DR, were also included in these differentially expressed miRNAs. Several miRNAs (let-7, miR-17, miR-29, miR-148, and miR-219) were predicted to target collagen synthesis (Table S3). In these miRNAs that target collagen synthesis, we focused on miR-29. Several targeting genes of miR-29, including CDC42, CDK6, COL1A1, DNMT3A, DNMT3B, IGF1, MCL1, and MMP2, have been confirmed so far via *in vitro* studies, and miR-29 was shown to modulate expressions of ECM components.²¹

As the elevated level of Col IV in retina of STZ-induced diabetic mice, we next set out to examine whether miR-29 targets Col IV. Strikingly, all members of the miR-29 family (miR-29a/b/c) contained binding sites in the 3' UTR of all Col IV transcripts. Interestingly, all members of the miR-29 family also target all Col I transcripts. However, other miRNAs, including the let-7 family, miR-20a/b, miR-20a/b/c, and miR-148a/b, only had potential binding sites for partial transcripts of Col I and Col IV (Table S4). We found two highly conserved binding sites for miR-29 in the 3' UTR region of Col IV A1 (Col4a1) in

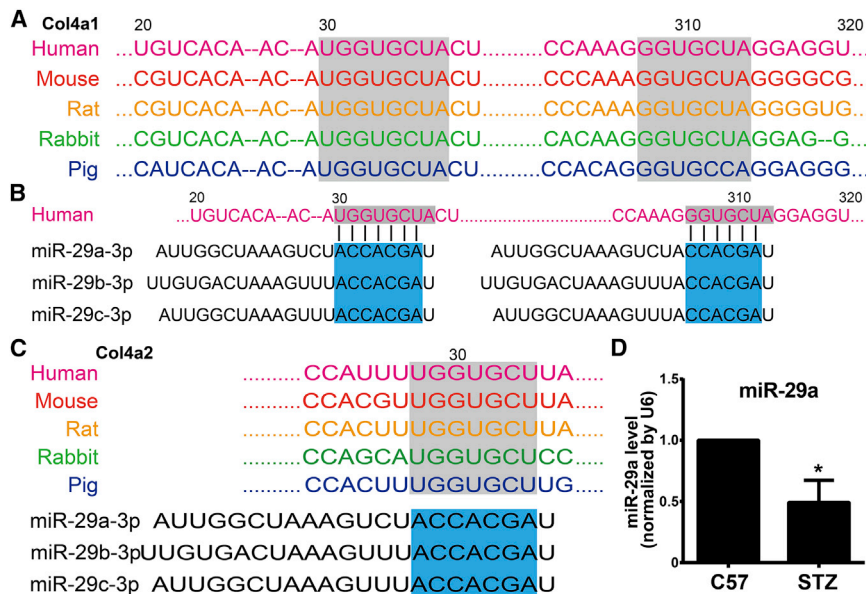


Figure 3. Predicted Binding Sites for miR-29 in the 3' UTR of Collagen Transcripts

(A) Predicted two binding sites for miR-29 in the Col4a1 3' UTR regions (30–37 and 308–314, shown in the gray boxes) are highly conserved in several species. (B) The three members of miR-29 family (miR-29a/b/c) contain binding sites in the 3' UTR of the Col4a1 transcript. The seed regions of the miR-29 family (shown in the blue boxes) are complementary to binding sites in the 3' UTR of the Col4a1 transcript. (C) Only one binding site in the 3' UTR of the Col IV A2 (Col4a2) transcript is found and complementary to the seed regions of the miR-29 family. (D) The expressions of miR-29a in retina of C57 and STZ-induced diabetic mice were examined by quantitative real-time PCR. N = 4 per group; *p < 0.05, STZ group versus control C57 group.

HRCECs, whereas a reduced mRNA level of Col IV was in the miR-29a mimic-transfected HRCECs (Figures 5A and 5B). Furthermore, we increased endogenous miR-29a expression by pre-miR-29a transfection. Similarly, quantitative real-time PCR analysis demonstrated that enhanced endogenous miR-29a expression resulted in a reduced mRNA level of Col IV in HRCECs (Figure 5C). Taken together, these findings suggest that miR-29a targets and downregulates Col IV expression in HRCECs.

OPN Upregulates Col IV Expression in HRCECs

Higher OPN levels in the vitreous fluid were found in patients with DR than in diabetic patients without DR. Consistent with these reports, the mRNA level of OPN was upregulated in retina of STZ-induced diabetic mice (Figure 6A). Strikingly, exogenous recombinant human (rh)OPN treatment resulted in increased mRNA and protein levels of Col IV in HRCECs (Figures 6B and 6C). Interestingly, exogenous rhOPN treatment also increased endogenous OPN expression in HRCECs (Figure 6C). Thus, we wondered whether OPN regulated the expression of Col IV. Overexpression of OPN by SPP1-OPN transfection resulted in increased OPN expression, with upregulated mRNA and protein levels of Col IV in HRCECs (Figures 6D–6F). Meanwhile, OPN small interfering (si)RNA transfection, which decreased the expression of OPN, resulted in downregulated mRNA and protein levels of Col IV in HRCECs (Figures 6G–6I). These findings indicate that OPN regulates Col IV expression in HRCECs.

OPN Regulates Col IV Expression via Repressing miR-29a

Next, we set out to explore the mechanism how OPN regulates the expression of Col IV. As nuclear factor κ B (NF- κ B)-response miR-29 regulates expression of Col IV in HRCECs and the role of OPN in inflammation and diabetes, we wondered whether OPN regulated Col IV expression via miR-29a. First, we examined the expres-

sion of OPN, Col IV, and miR-29a in HRCECs under HG conditions. Compared with normal glucose conditions (5.5 mM glucose), 30 mM HG conditions resulted in significantly elevated mRNA levels of OPN, Col IV, and miR-29a in HRCECs (Figures 7A–7C). Furthermore, exogenous rhOPN treatment and overexpression of OPN by SPP1-OPN transfection decreased mRNA levels of miR-29a in HRCECs (Figures 7D and 7E). In contrast, OPN-siRNA transfection upregulated the mRNA level of miR-29a in HRCECs (Figure 7F). These results indicate that OPN represses miR-29a expression in HRCECs.

To examine further the role of miR-29a in OPN-regulated Col IV expression, we transfected HRCECs with pre-miR-29a to upregulate endogenous miR-29a and then treated HRCECs with exogenous rhOPN. Quantitative real-time PCR analysis showed that an elevated miR-29a level by pre-miR-29a transfection was reversed by exogenous rhOPN treatment (Figure 7G). As a result, reduced mRNA and protein levels of Col IV by pre-miR-29a transfection were reversed by exogenous rhOPN treatment (Figures 7H and 7I). Taken together, these findings demonstrate that OPN upregulates Col IV expression through a miR-29a-repressed pathway.

DISCUSSION

Diabetic retinopathy, a microcirculation disturbance triggered by a persistent high level of blood glucose, is a multifactorial and complicated illness with abnormality of vessel in retina. A main hallmark of DR is the thickening of retinal capillary BMs. The human retinal capillary BMs included four Col IV (a1/2/3/4, 12.7% of the total ECM) and three collagen VI (3.6%) peptide chains, five laminin peptide chains (24.6%), perlecan (9.6%), agrin (3.2%), biglycan (3.8%), and so on. All ECM proteins found in nondiabetic retinal capillary BMs were also detected in capillary BMs of diabetic donors. However, retinal capillary BMs of diabetic patients contain a series of proteins that were undetected in BMs of nondiabetic donors, such as two members of the complement family (C4 and C9).²² Members of collagen families IV, VI, and XVIII have elevated abundance in

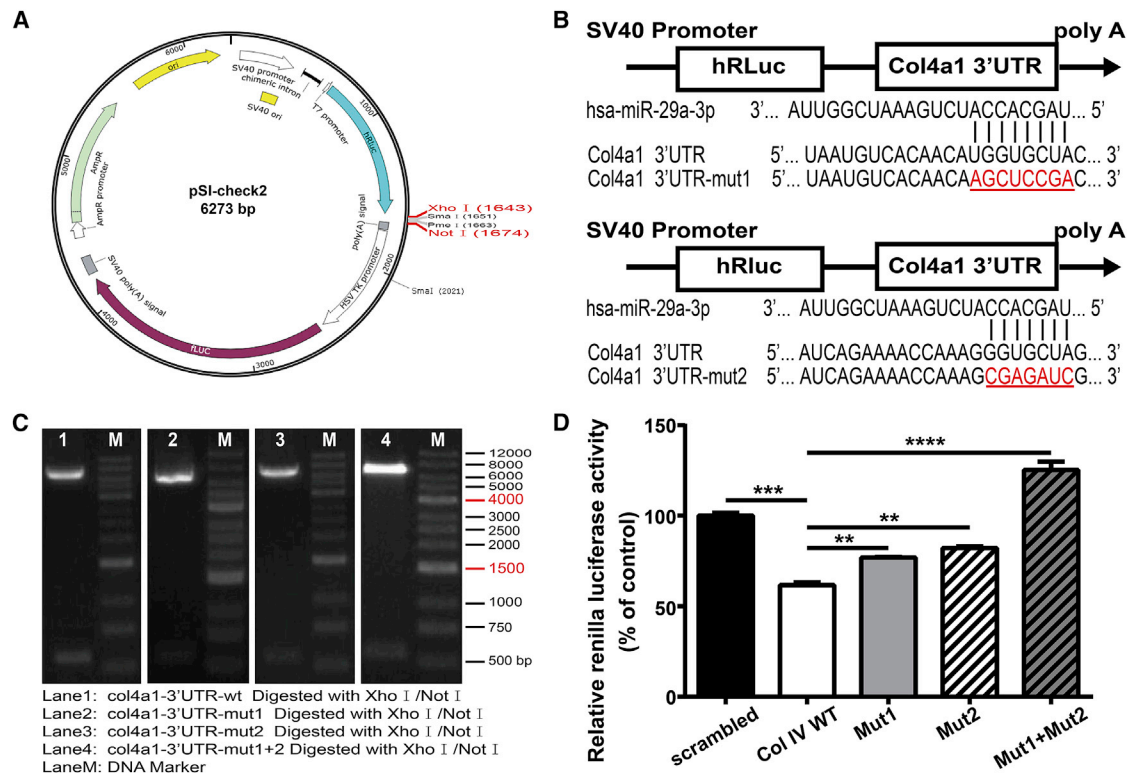


Figure 4. miR-29a Directly Binds the 3' UTR Binding Sites and Inhibited Col4a1 Expression

(A) The 3' UTR of Col4a1 was cloned downstream of the human renilla luciferase reporter (hRLuc) of the pSI-check2 vector. (B) The wild-type (WT) and mutant sequences of Col4a1 3' UTR (red and underlined). For Mut1 + Mut2, both Col4a1 3' UTR mutants (Mut1 and Mut2) were included. (C) The wild-type and mutant sequences of Col4a1 3' UTR, digested by restriction enzymes XhoI/NotI, were further confirmed by DNA sequence. (D) HEK293T cells were cotransfected with miR-29a (or scrambled miRNA) and WT or the mutant Col4a1 3' UTR-pSI-check2 vector. After 48 h, cells were lysed, and luciferase activity was detected. N = 3 per group; **p < 0.01, ***p < 0.001, and ****p < 0.0001.

diabetic BMs.²² Meanwhile, Col IV levels in serum and vitreous fluid were also found to be higher in diabetic patients with DR than in those without DR.⁸ Similarly, compared with diabetic patients without DR, higher levels of OPN in serum and vitreous fluid were found in patients with DR.¹⁴ A previous study demonstrated that upregulation of OPN in HRCECs under high glucose conditions induces endothelial cell proliferation and retinal neo-capillarization.²³ Thus, these studies suggest that OPN may play an important role in the pathogenesis of DR. In the present study, we explored the role of OPN in the thickening of retinal capillary BMs. We found that high glucose induced elevated levels of OPN and Col IV, and OPN upregulated expression of Col IV (the main retinal capillary BM protein) in HRCECs. Interestingly, a previous study has shown that laminin, another main retinal capillary BM protein, reduced in diabetic BMs.²² Whether high glucose induces a reduced level of laminin and whether OPN also involves the reduced level of laminin need further examinations.

Recently, with the use of HRCECs and RPE cells *in vitro* and STZ-induced diabetic mice *in vivo*, numerous studies have investigated the roles of miRNAs in DR. A number of miRNAs were found to play crit-

ical roles in the progression of DR, including miR-17, miR-18, miR-20, miR-21, miR-31, miR-34, miR-146, and miR-155 and so on. Herein, with the use of small RNA sequencing technology, we identified a series of differentially expressed small RNAs in retinas between control C57 and STZ-induced mice. We found 51 differentially expressed miRNAs, with 42 miRNAs upregulated and 9 downregulated. Among these differentially expressed miRNAs, 11 miRNAs are novel, and 40 miRNAs have been identified, including several miRNAs (miR-10, miR-17, miR-34, miR-144, miR-190, miR-199, miR-200, miR-216, and miR-219) that have been proved to be involved in DR.¹⁷ By screening databases, we paid attention to miR-29 and examined its role in the upregulation of Col IV, as all members of the miR-29 family targeted 3' UTR of several main collagen transcripts in retinal capillary BMs. In the present results, we confirmed that Col IV transcripts are the targets of miR-29a, and OPN upregulated the expression of Col IV via repressing miR-29a in HRCECs. Suppression of collagen expression by miR-29 has also been reported in other cells and tissues, e.g., renal tubular epithelial cells, hepatic stellate cells, and trabecular meshwork.^{24,25} In DN, another serious complication confronted by diabetes, downregulated miR-29 is negatively correlated with both serum creatinine and creatinine clearance.²⁶ In retinopathy of prematurity

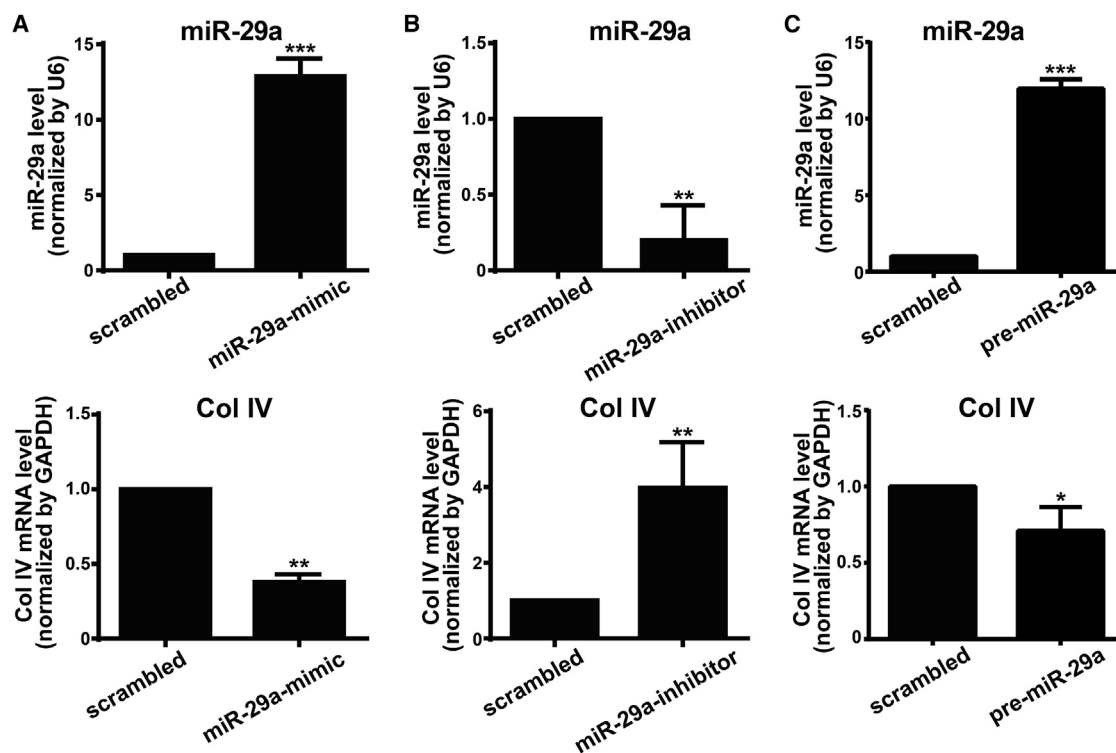


Figure 5. miR-29a Regulates Col IV Expression in HRCECs

HRCECs were transfected with miR-29 mimic (A), miR-29 inhibitor (B) or pre-miR-29a (C), as well as respective scrambled control for 72 h. mRNA levels of miR-29a and Col IV were determined by quantitative real-time PCR analysis. Data were presented as mean \pm SD. N = 3 per group; *p < 0.05, **p < 0.01, and ***p < 0.001.

(ROP), miR-29a was found to inhibit retinal neo-capillarization and prevent the development and progression of ROP by downregulating angiotensinogen.²⁷ These studies suggest that miR-29 exhibits diverse roles in capillary complication of diabetes, and miR-29 is a novel marker in the pathogenesis of DR. Furthermore, a number of miRNAs that were differentially expressed in STZ-induced diabetic mice, but their functions were not reported, were identified by small RNAs sequencing technology, and their roles in pathogenesis of DR need further studies.

Increased expression of OPN was demonstrated in several chronic inflammatory diseases, such as atherosclerosis, indicating inflammation as a link between OPN and DR.²⁸ OPN is expressed by inflammatory cells, such as macrophages, and highly induced during inflammatory activation.²⁹ Meanwhile, OPN modulates the inflammatory response at several levels, from immune cell accumulation to activation of T helper cell type 1 (Th1) cytokines and to cell survival, thus exacerbating the chronic inflammatory response.¹¹ NF- κ B was a key transcription factor that was induced by tumor necrosis factor alpha (TNF- α), which played an important role in regulating inflammation and was reported to participate in the pathological progression of DR. The activation of NF- κ B was also confirmed in both human diabetic patients and animal models of diabetes. Recent works showed that NF- κ B played an important role during lipopolysaccharide (LPS)-stimulated OPN expression.³⁰ In turn, OPN also enhanced NF- κ B activation through phosphorylation and degradation of inhibitor of κ B (I κ B),³¹ and

OPN receptor integrin α v β 3 and its downstream SFK (Src family of tyrosine kinases) were required for NF- κ B activation.³² A previous study demonstrated that miR-21, miR-132, miR-146, and miR-155 were NF- κ B responsive in diabetic HRCECs.¹⁷ Interestingly, NF- κ B was also demonstrated to regulate miR-29 expression.³³ Furthermore, miR-29c was reported to promote an inflammatory response under hyperglycemic conditions by directly targeting tristetraprolin (TTP).³⁴ In the present study, OPN inhibited the expression of miR-29a in HRCECs. The unknown pathway or factors that mediate the repression of miR-29a by OPN need further exploration, and NF- κ B might be a potential transcription factor involved in these effects.

In summary, this study demonstrates that miR-29a was a mediator that was involved in the OPN-induced upregulation of the main ECM protein Col IV in HRCECs. These findings provide the molecular mechanism of regulation of OPN and miR-29a in the abnormal expression of Col IV and the thickening of capillary BMs in DR and indicate that OPN and miR-29a may be potential biomarkers of DR and provide new targets for DR treatment.

MATERIALS AND METHODS

Development of an Animal Model of Diabetes

The 8-week-old male C57BL/6 mice used in the present study were obtained from Experimental Animal Institute of the Third Military Medical University (Amy Medical University). These animals were

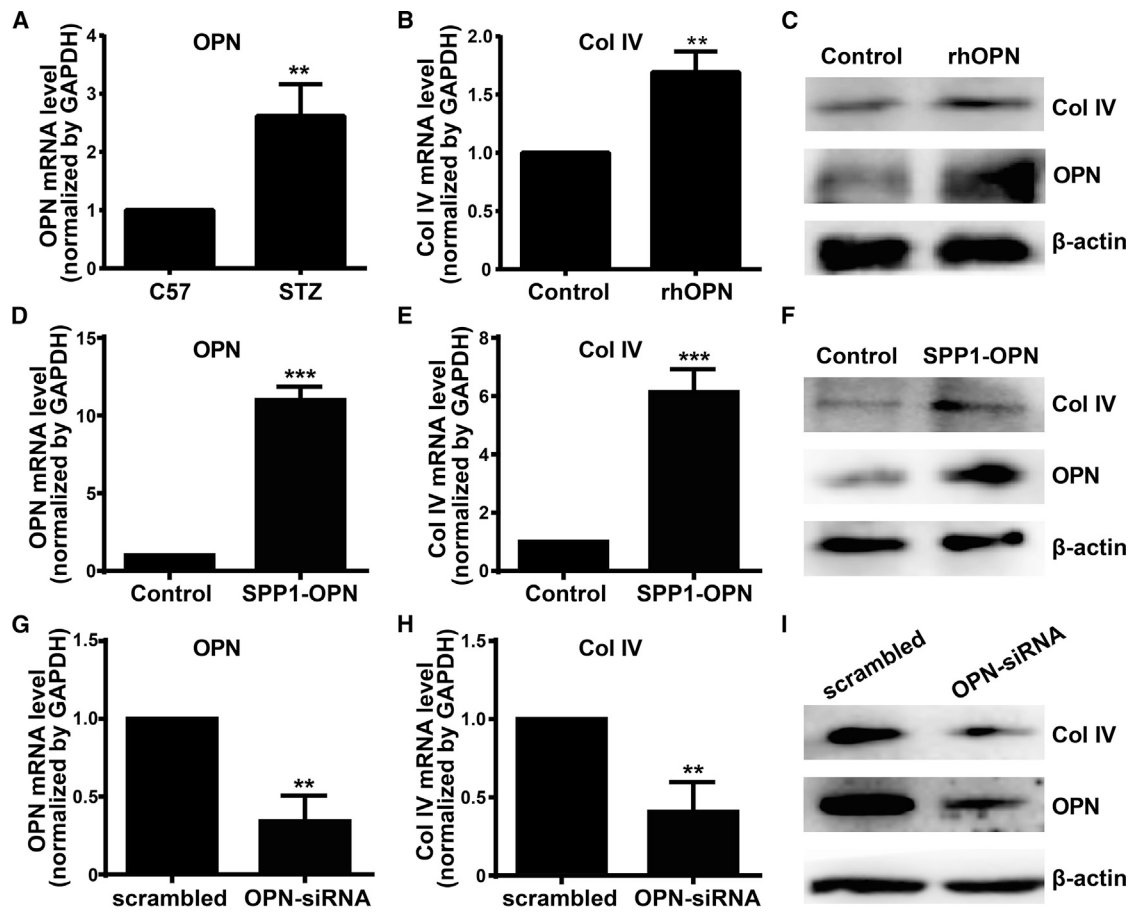


Figure 6. OPN Upregulates Col IV Expression in HRCECs

(A) The expressions of OPN in retinas of C57 and STZ-induced diabetic mice were examined by quantitative real-time PCR. (B and C) mRNA and protein levels of Col IV in HRCECs after exogenous rhOPN (400 ng/mL) treatment for 48 h. (D–F) HRCECs were transfected with SPP1-OPN, as well as respective scrambled control for 72 h. mRNA and protein levels of OPN and Col IV were determined by quantitative real-time PCR and western blotting analysis. (G–I) HRCECs were transfected with OPN-siRNA, as well as respective scrambled control for 72 h. mRNA and protein levels of OPN and Col IV were determined by quantitative real-time PCR and western blotting analysis. Data were presented as mean \pm SD. N = 3 per group; ** $p < 0.01$ and *** $p < 0.001$.

housed in a controlled environment with standard conditions of temperature and humidity with a cycle of an alternating 12-h light and dark. The animal protocols were conducted with the approval of and in accordance with the relevant guidelines and regulations of the Third Military Medical University (Army Medical University), Chongqing, China. These mice were randomly divided into two groups: control C57 and STZ groups. Prior to STZ injection, no significant differences in blood glucose level or body weight were noted between the two groups. The model of diabetes was induced by intraperitoneal injection of 60 mg/mL STZ (Sigma-Aldrich) in 0.1 M citrate buffer for 5 consecutive days. Mice in the control C57 group received citrate buffer only. The blood glucose concentration was examined with an Accu-Chek Active glucometer (Roche) glucose analyzer, and successful diabetic mice had a greater than 11.1-mL blood glucose concentration. STZ mice with sustained blood glucose increase for 3 months were included in follow-up experiments.

FFA and TEM

After 3 months, FFA and TEM were used to observe the structural changes of STZ mice's eyes. After fluorescein sodium was injected intraperitoneally, the dilated pupils of anesthetized mice were examined by FFA, performed using a digital fundus camera (Model TRC 50 IA; Topcon). To minimize observer variations, all scans were performed by the same experienced physician. For TEM, after the anterior segment and crystalline lens were removed, retinas were detached and separated from the optic nerve head. The dissected retinas were immediately fixed in 2.5% glutaraldehyde solution in 0.1 M phosphate buffer (PBS, pH 7.4) for 24 h. After three washes in PBS and dehydration in an ethanol and propylene oxide series, retinas were then embedded in an Epon812 mixture at 37°C for 3 h. After polymerization at 60°C for 24 h, ultrathin sections (50–60 nm) were obtained with an ultra-microtome (MT-X; RMC) and then collected on 100 mesh copper grids. After staining with 2% uranyl acetate (15 min) and lead citrate (5 min), the sections were visualized using TEM.

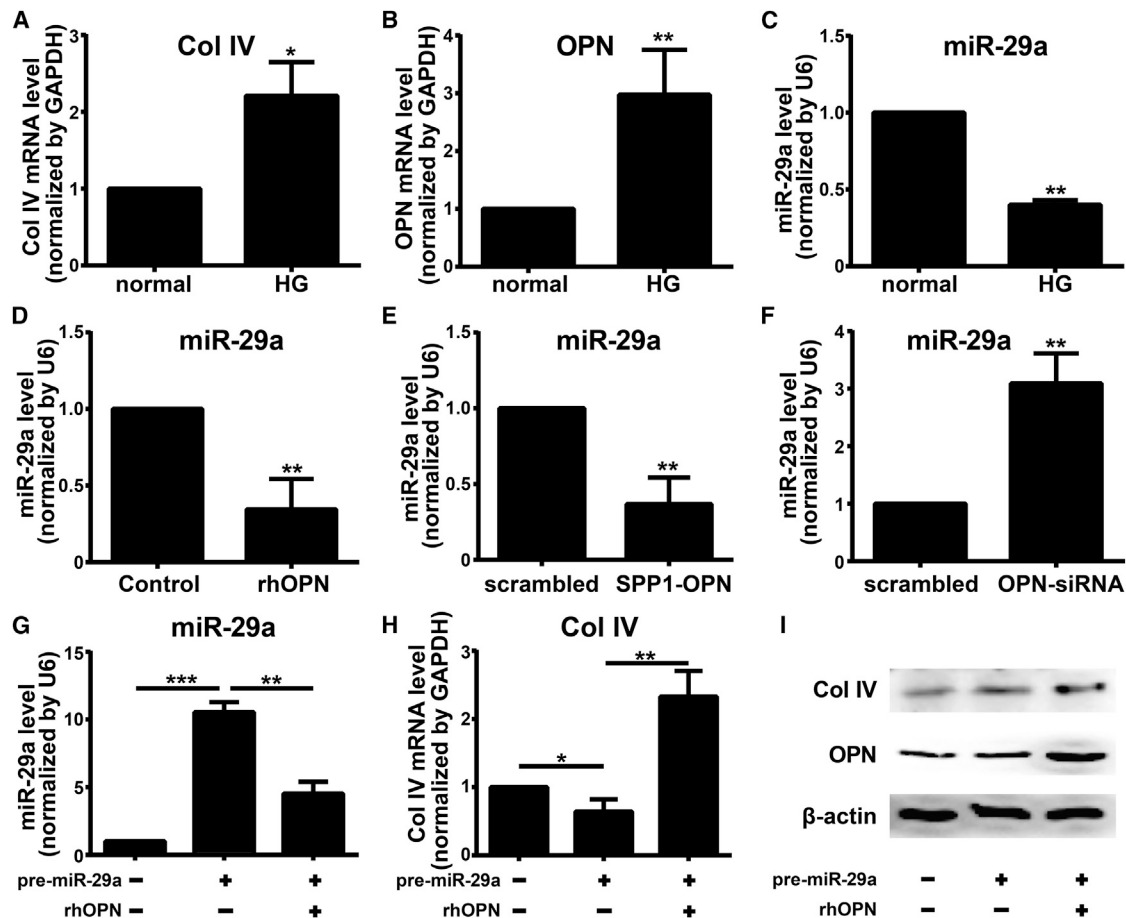


Figure 7. OPN Regulates Col IV Expression by Repressing miR-29a

(A–C) mRNA levels of Col IV (A), OPN (B), and miR-29a (C) in HRCECs under normal and high glucose (HG) conditions. (D–F) mRNA levels of miR-29a in HRCECs after exogenous rhOPN treatment (D; 400 ng/mL, 48 h), SPP1-OPN transfection (E), and OPN-siRNA transfection (F). (G–I) HRCECs were transfected with pre-miR-29a and then treated with exogenous rhOPN. mRNA levels of miR-29a (G) and Col IV (H) in HRCECs were assessed by quantitative real-time PCR analysis. Protein level of Col IV in HRCECs was assessed by western blotting (I). Data were presented as mean \pm SD. N = 3 per group; * p < 0.05, ** p < 0.01, and *** p < 0.001.

Retina Whole-Mount and PAS Staining

The 3-month-old STZ mice's eyes were placed in formaldehyde solution and fixed for 20 min. The entire retinas were carefully dissected using forceps. The retinas were incubated in 1 g/L protease K at 56°C for 15 min. After wash, retinas were further incubated in 3% trypsin at 37°C for 40–60 min. The preparations were radially cut toward the optic nerve head, flat mounted onto glass slides, and air dried. The retinas were further stained with PAS stain and hematoxylin to evaluate retina microcapillary morphology.

RNA Isolation and Quantitative Real-Time PCR

Total RNA from tissues (3 months after STZ injection) or cells was isolated as described by the manufacturer (TRIzol; Invitrogen). RNA was treated with RQ1 RNase-free DNase I (Promega) to remove DNA contaminants. The concentration and purity of RNA were assessed by spectrophotometry. RNAs (10 ng) were reverse transcribed into cDNA, and quantitative real-time PCR was performed on a Bio-Rad SYBR Green PCR Master Mix (Bio-Rad). The final volume

of the PCR reaction mixture was 20 μ L that contained 2 μ L cDNA, 1 μ M of each primer, 10 μ L GoTaq qPCR Master Mix (Promega), and sterile water up to 20 μ L. For miRNA quantitative real-time PCR, miRNAs were reverse transcribed, and quantitative real-time PCR was performed according to miRNA First Strand cDNA Synthesis (Sangon Biotech, Shanghai, China). Primers of miR-29 were selected and purchased from the GeneGlobe Search Center (QIAGEN). Primers used in this study were shown in Table S5. Relative mRNA levels of Col IV and OPN were normalized to the level of glyceraldehyde 3-phosphate dehydrogenase (GAPDH), and the relative miR-29 level was normalized to RNU6 (U6) of the same sample.

Small RNA Sequencing and miRNA Target Prediction

Small RNAs of control C57 and STZ-induced diabetic retina samples (3 months after STZ injection) were sequenced by using BGISEQ-500 technology in the Beijing Genomics Institute (BGI; China). The small RNA expression level is calculated by using transcript parts per million (TPM). DES screening is performed to find differentially

expressed small RNAs between samples and to do further analysis. In order to find the possible targets, multiple software, including RNAhybrid, miRanda, miRBase, and TargetScan, was used. Additionally, we performed GO enrichment analysis and pathway enrichment analysis of these screened DES target genes based on the KEGG database. Sequencing datasets were deposited to NCBI-Sequence Read Archive (SRA; NCBI: SRX6870744, SRX6870745, SRX6870746, SRX6870747, SRX6870748, and SRX6870749).

Cell Cultures

HRCECs were purchased from the BeNa Culture Collection (BNCC339792; Beijing, China). HRCECs were cultured in Dulbecco's modified Eagle medium/F-12 (DMEM/F-12; Hyclone) containing 5% fetal bovine serum (FBS; Gibco) and 1% endothelial cell growth supplement (ScienCell). HRCEC cultures were maintained at 37°C in a humidified atmosphere containing 5% CO₂.

Western Blotting

Protein samples were reconstituted in sample buffer and denatured by boiling at 100°C for 5 min. Protein lysates were loaded on 8%–10% SDS-PAGE for electrophoresis and electrophoretic transferred onto a methanol-activated polyvinylidene difluoride (PVDF) membrane (0.45 µm; Millipore). Nonspecific protein was blocked by incubation with 5% BSA for 1 h at room temperature. The membrane was probed by mouse monoclonal anti-β-actin antibody (Abcam; ab82226), rabbit polyclonal anti-OPN antibody (Abcam; ab8448), and rabbit polyclonal anti-Col IV (Abcam; ab6586) at 4°C for 16 h. The target proteins were recognized by horseradish peroxidase (HRP)-conjugated secondary antibodies (Abcam; ab6789 and ab205718) by 2 h incubation at room temperature. The immunoreactive bands were presented by reacting with chemiluminescence reagents (enhanced chemiluminescence [ECL]; Pierce).

Transfection

miRNA mimic- miR-29a (miR-29a mimic), miR-29a inhibitor, and scrambled miRNA control were obtained from Sangon Biotech (Shanghai, China). HRCECs were seeded in 6-well plates, incubated overnight to a density of 90%, and transfected using Lipofectamine 3000 (Thermo Fisher Scientific) for 72 h as instructed. For pre-miR-29a transfection, HRCECs were transfected at 50% to 70% confluence with human pre-miR-29a (50 nM) or pre-miRNA negative control (50 nM; Shanghai GenePharma, China) lentivirus for 72 h as instructed. To achieve alteration of OPN expression, HRCECs were transfected at 50% to 70% confluence with SPP1-OPN or OPN-siRNA adenovirus for 72 h. Afterward, medium was replaced with fresh medium for subsequent protein or RNA analyses, respectively.

Plasmid Constructs and Luciferase Reporter Assay

The 3' UTR of the Col4a1 transcript bearing putative binding sites for miR-29a was from Sangon Biotech (Shanghai, China). Furthermore, the wild-type putative binding sites of Col4a1, as well as the three corresponding mutants, were cloned downstream of the renilla luciferase reporter of the pSI-check2 vector (Figures 4A and 4B). For reporter assays, HEK293T cells with 50%–70% confluence in 96-well plates

were transfected using Lipofectamine 3000 by 500 nM hsa-miR-29a-3p (or scrambled control) and 16 µg/mL pSI-check2 vector (wild-type or mutant 3' UTR of Col4a1). The level of miR-29a in HEK293T cells was analyzed by quantitative real-time PCR, demonstrating stable levels between 6 h and 48 h after transfection. Cells were therefore harvested 48 h after transfection, and luciferase activity was determined using the Dual Luciferase Reporter Assay System (Promega), according to the manufacturer's recommendations. The luciferase reporter activity was determined by the human renilla luciferase reporter (hRluc) luminescence measurement normalized to firefly luminescence (human luciferase reporter [hLuc]). All samples were measured in triplicate, and experiments were performed three times.

Statistical Analysis

The data were shown as mean ± SD. Statistical analysis was conducted with SPSS 15.0 software using the paired Student's t test for comparisons of two groups or one-way ANOVA for multiple group comparisons. $p < 0.05$ was considered statistically significant.

SUPPLEMENTAL INFORMATION

Supplemental Information can be found online at <https://doi.org/10.1016/j.omtn.2020.02.001>.

AUTHOR CONTRIBUTIONS

P.D. designed the experiments and prepared the manuscript. S.C. and Y.Z. conducted the experiments and analyzed the data. H.X. and Y.L. critically reviewed and revised the manuscript and assisted with the discussion. All authors critiqued the manuscript and approved its submission.

CONFLICTS OF INTEREST

The authors declare no competing interests.

ACKNOWLEDGMENTS

We thank Yijian Li for his preparation of the graphic scheme summarizing our present study. This work was supported by grants from the National Science Foundation of China (8140030635, 81400418, and 81470671).

REFERENCES

- Cheung, N., Mitchell, P., and Wong, T.Y. (2010). Diabetic retinopathy. *Lancet* 376, 124–136.
- Roy, S., Ha, J., Trudeau, K., and Beglova, E. (2010). Vascular basement membrane thickening in diabetic retinopathy. *Curr. Eye Res.* 35, 1045–1056.
- To, M., Goz, A., Camenzind, L., Oertle, P., Candiello, J., Sullivan, M., Henrich, P.B., Loparic, M., Safi, F., Eller, A., and Halfter, W. (2013). Diabetes-induced morphological, biomechanical, and compositional changes in ocular basement membranes. *Exp. Eye Res.* 116, 298–307.
- Halfter, W., Candiello, J., Hu, H., Zhang, P., Schreiber, E., and Balasubramani, M. (2013). Protein composition and biomechanical properties of in vivo-derived basement membranes. *Cell Adhes. Migr.* 7, 64–71.
- Uechi, G., Sun, Z., Schreiber, E.M., Halfter, W., and Balasubramani, M. (2014). Proteomic View of Basement Membranes from Human Retinal Blood Vessels, Inner Limiting Membranes, and Lens Capsules. *J. Proteome Res.* 13, 3693–3705.

6. Banu, N., Hara, H., Egusa, G., and Yamakido, M. (1994). Serum and urinary type IV collagen concentrations in the assessment of diabetic microangiopathy. *Hiroshima J. Med. Sci.* 43, 123–133.
7. Yagame, M., Suzuki, D., Jinde, K., Saotome, N., Sato, H., Noguchi, M., Sakai, H., Kuramoto, T., Sekizuka, K., Iijima, T., et al. (1997). Significance of urinary type IV collagen in patients with diabetic nephropathy using a highly sensitive one-step sandwich enzyme immunoassay. *J. Clin. Lab. Anal.* 11, 110–116.
8. Kotajima, N., Kanda, T., Yuuki, N., Kimura, T., Kishi, S., Fukumura, Y., Tamura, I., and Kobayashi, I. (2001). Type IV collagen serum and vitreous fluid levels in patients with diabetic retinopathy. *J. Int. Med. Res.* 29, 292–296.
9. Mundel, T.M., and Kalluri, R. (2007). Type IV collagen-derived angiogenesis inhibitors. *Microvasc. Res.* 74, 85–89.
10. Butler, W.T. (1989). The nature and significance of osteopontin. *Connect. Tissue Res.* 23, 123–136.
11. Kahles, F., Findeisen, H.M., and Bruemmer, D. (2014). Osteopontin: A novel regulator at the cross roads of inflammation, obesity and diabetes. *Mol. Metab.* 3, 384–393.
12. Yamaguchi, H., Igarashi, M., Hirata, A., Tsuchiya, H., Sugiyama, K., Morita, Y., Jimbu, Y., Ohnuma, H., Daimon, M., Tominaga, M., and Kato, T. (2004). Progression of diabetic nephropathy enhances the plasma osteopontin level in type 2 diabetic patients. *Endocr. J.* 51, 499–504.
13. Zhang, X., Chee, W.K., Liu, S., Tavintharan, S., Sum, C.F., Lim, S.C., and Kumari, N. (2018). Association of plasma osteopontin with diabetic retinopathy in Asians with type 2 diabetes. *Mol. Vis.* 24, 165–173.
14. Abu El-Asrar, A.M., Imtiaz Nawaz, M., Kangave, D., Siddiquei, M.M., and Geboes, K. (2012). Osteopontin and other regulators of angiogenesis and fibrogenesis in the vitreous from patients with proliferative vitreoretinal disorders. *Mediators Inflamm.* 2012, 493043.
15. Sodhi, C.P., Phadke, S.A., Battle, D., and Sahai, A. (2001). Hypoxia and high glucose cause exaggerated mesangial cell growth and collagen synthesis: role of osteopontin. *Am. J. Physiol. Renal Physiol.* 280, F667–F674.
16. Nicholas, S.B., Liu, J., Kim, J., Ren, Y., Collins, A.R., Nguyen, L., and Hsueh, W.A. (2010). Critical role for osteopontin in diabetic nephropathy. *Kidney Int.* 77, 588–600.
17. Gong, Q., and Su, G. (2017). Roles of miRNAs and long noncoding RNAs in the progression of diabetic retinopathy. *Biosci. Rep.* 37, BSR20171157.
18. Yan, B., Tao, Z.F., Li, X.M., Zhang, H., Yao, J., and Jiang, Q. (2014). Aberrant expression of long noncoding RNAs in early diabetic retinopathy. *Invest. Ophthalmol. Vis. Sci.* 55, 941–951.
19. Bartel, D.P. (2009). MicroRNAs: target recognition and regulatory functions. *Cell* 136, 215–233.
20. Roy, S., Maiello, M., and Lorenzi, M. (1994). Increased expression of basement membrane collagen in human diabetic retinopathy. *J. Clin. Invest.* 93, 438–442.
21. Du, B., Ma, L.M., Huang, M.B., Zhou, H., Huang, H.L., Shao, P., Chen, Y.Q., and Qu, L.H. (2010). High glucose down-regulates miR-29a to increase collagen IV production in HK-2 cells. *FEBS Lett.* 584, 811–816.
22. Halfter, W., Moes, S., Asgeirsson, D.O., Halfter, K., Oertle, P., Melo Herraiz, E., Plodinec, M., Jenoe, P., and Henrich, P.B. (2017). Diabetes-related changes in the protein composition and the biomechanical properties of human retinal vascular basement membranes. *PLoS ONE* 12, e0189857.
23. Huang, Q., and Sheibani, N. (2008). High glucose promotes retinal endothelial cell migration through activation of Src, PI3K/Akt1/eNOS, and ERKs. *Am. J. Physiol. Cell Physiol.* 295, C1647–C1657.
24. Kwiecinski, M., Noetel, A., Elfimova, N., Trebicka, J., Schievenbusch, S., Strack, I., Molnar, L., von Brandenstein, M., Töx, U., Nischt, R., et al. (2011). Hepatocyte growth factor (HGF) inhibits collagen I and IV synthesis in hepatic stellate cells by miRNA-29 induction. *PLoS ONE* 6, e24568.
25. Villarreal, G., Jr., Oh, D.J., Kang, M.H., and Rhee, D.J. (2011). Coordinated regulation of extracellular matrix synthesis by the microRNA-29 family in the trabecular meshwork. *Invest. Ophthalmol. Vis. Sci.* 52, 3391–3397.
26. Zhou, L., Xu, D.Y., Sha, W.G., Shen, L., Lu, G.Y., Yin, X., and Wang, M.J. (2015). High glucose induces renal tubular epithelial injury via Sirt1/NF-kappaB/microR-29/Keap1 signal pathway. *J. Transl. Med.* 13, 352.
27. Chen, X.K., Ouyang, L.J., Yin, Z.Q., Xia, Y.Y., Chen, X.R., Shi, H., Xiong, Y., and Pi, L.H. (2017). Effects of microRNA-29a on retinopathy of prematurity by targeting AGT in a mouse model. *Am. J. Transl. Res.* 9, 791–801.
28. Lund, S.A., Giachelli, C.M., and Scatena, M. (2009). The role of osteopontin in inflammatory processes. *J. Cell Commun. Signal.* 3, 311–322.
29. Lund, S.A., Wilson, C.L., Raines, E.W., Tang, J., Giachelli, C.M., and Scatena, M. (2013). Osteopontin mediates macrophage chemotaxis via $\alpha 4$ and $\alpha 9$ integrins and survival via the $\alpha 4$ integrin. *J. Cell. Biochem.* 114, 1194–1202.
30. Zhao, W., Wang, L., Zhang, M., Wang, P., Zhang, L., Yuan, C., Qi, J., Qiao, Y., Kuo, P.C., and Gao, C. (2011). NF- κ B- and AP-1-mediated DNA looping regulates osteopontin transcription in endotoxin-stimulated murine macrophages. *J. Immunol.* 186, 3173–3179.
31. Das, R., Philip, S., Mahabeshwar, G.H., Bulbule, A., and Kundu, G.C. (2005). Osteopontin: it's role in regulation of cell motility and nuclear factor kappa B-mediated urokinase type plasminogen activator expression. *IUBMB Life* 57, 441–447.
32. Courter, D.L., Lomas, L., Scatena, M., and Giachelli, C.M. (2005). Src kinase activity is required for integrin α V β 3-mediated activation of nuclear factor-kappaB. *J. Biol. Chem.* 280, 12145–12151.
33. Wang, H., Garzon, R., Sun, H., Ladner, K.J., Singh, R., Dahlman, J., Cheng, A., Hall, B.M., Qualman, S.J., Chandler, D.S., et al. (2008). NF-kappaB-YY1-miR-29 regulatory circuitry in skeletal myogenesis and rhabdomyosarcoma. *Cancer Cell* 14, 369–381.
34. Guo, J., Li, J., Zhao, J., Yang, S., Wang, L., Cheng, G., Liu, D., Xiao, J., Liu, Z., and Zhao, Z. (2017). MiRNA-29c regulates the expression of inflammatory cytokines in diabetic nephropathy by targeting tristetraprolin. *Sci. Rep.* 7, 2314.